https://doi.org/10.1595/205651322X16260797478755 *Johnson Matthey Technol. Rev.*, 2022, **66**, (1), 32–43

JOHNSON MATTHEY
TECHNOLOGY REVIEW

www.technology.matthey.com

Comparative Study of Radiative Heating Techniques for Fast Processing of Functional Coatings for Sustainable Energy Applications

Applications of radiative mechanisms in solar energy, battery storage and fuel cells

Rebecca Griffin, Katherine Hooper, Cecile Charbonneau, Jenny Baker*
Faculty of Science and Engineering, SPECIFIC, Swansea University Bay Campus, Fabian Way, Crymlyn Burrows, Swansea, SA1 8EN, UK

***Email:** j.baker@swansea.ac.uk

PEER REVIEWED

Received 26th March 2021; Revised 9th July 2021; Accepted 12th July 2021; Online 12th July 2021

This study assesses the use of short wavelength radiative heating techniques such as near infrared (NIR), intense pulsed light (IPL) and ultraviolet (UV) heating for processing coatings in energy applications. It concentrates on the importance of investigating different radiative wavelengths to advance these technologies as scalable processes *via* reduced heating times. It illustrates the mechanisms by which these techniques can transform thin film materials: sintering, binder removal, drying and chemical reactions. It focuses on successful research applications and the methods used to apply these radiative mechanisms in solar energy, battery storage and fuel cells, while considering the materials suitable for such intentions. The purpose of this paper is to highlight to academics as well as industrialists some of the potential advantages and applications of radiative heating technologies.

1. Introduction

The drive to reduce carbon emissions in order to meet the national commitments on climate change, including the recent requirement 'net zero' (1) put into law by the UK Government, has led to increased demand for electrical energy harvesters and energy storage (2–4). A large amount of research has been undertaken in developing batteries, fuel cells and solar cells. The development of functional coatings has been critical for the advancement of these technologies which are supporting a transition to a low carbon economy. Academic advances have typically focused on new chemistries such as the development of lithium cobalt oxide as a cathode material to enable high energy density lithium-ion batteries (LIBs) (5) or lead halide perovskite (6, 7) for a solution processed photovoltaic (PV) application.

In order to commericalise a system the manufacturing method must be compatible with an industrial process otherwise the cost will be prohibitive for all but niche applications. While there is much focus on printing and coating speed for roll-to-roll production (8, 9), the factor limiting line speed is often drying or curing time rather than the speed of coating. For example, slot die coating can operate at speeds >100 m min^{-1} (10). If the drying time is 10 min this will require an oven of 1 km for the line to run at maximum coating speed. In reality the system is often optimised around the drying system.

This study focuses on fast heating techniques for energy applications, such as PV, batteries and

fuel cells, with coating thickness in the range of 50 nm to 500 µm. Fast heating techniques for the purposes of this study are defined as heating techniques that aim to directly heat the material through a radiative method (with wavelengths less than 2500 nm) (**Figure 1**) rather than conventional heating technologies such as hot air ovens where heat is transferring *via* a combination of convection, conduction and radiation. Due to the selective absorption of energy, these techniques can enable coatings to be heated to higher temperatures than the substrates can withstand. This is particularly apparent when sintering metallic materials on polymer substrates for flexible applications (11). Microwave heating is outside the scope of this review due to the differences in how the radiation interacts with the material being processed; a detailed review of microwave processing was undertaken by Oghbaei *et al*. (12).

In all cases considered (UV, IPL and NIR technologies illustrated in **Figure 2**) the material must absorb the emitted radiation. **Figure 2(a)** shows all of the UV radiation being absorbed within the coating initiating a chemical reaction such as crosslinking. In the case of IPL (**Figure 2(b)**), while some of the radiation is directly absorbed by the coating causing heating, some is reflected from the substrate and some is reflected on the top surface of the coating disseminating to the atmosphere. Some materials are transparent to NIR radiation as shown in **Figure 2(c)**, causing the radiation to pass through without heating, whereas other materials absorb or reflect the radiation. The amount of energy per square metre of the three techniques varies from 1200 kW m^{-2} for NIR which is applied for the order of seconds, to 49,000 kW m^{-2} for IPL which will be applied for only a few milliseconds. UV has a range between 800–4000 kW m^{-2}. The temperature achieved is highly dependent on the material being processed but typically NIR can achieve 800°C +, UV 2–300°C and IPL 200–300°C due to the short timeframe of operation.

If the material is transparent to the incoming radiation; for example in the case of soda lime glass under NIR (13), no heating occurs unless there is another coating in direct contact with the one to be heated, which does absorb the given wavelength. In some cases the material can be engineered by incorporating a material which absorbs more readily, such as carbon black, within

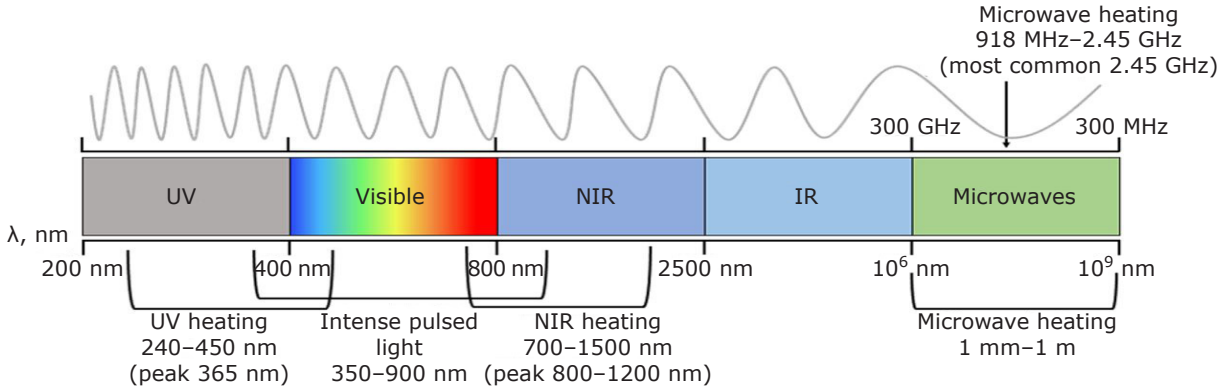

Fig. 1. Electromagnetic spectrum with different heating technologies highlighted

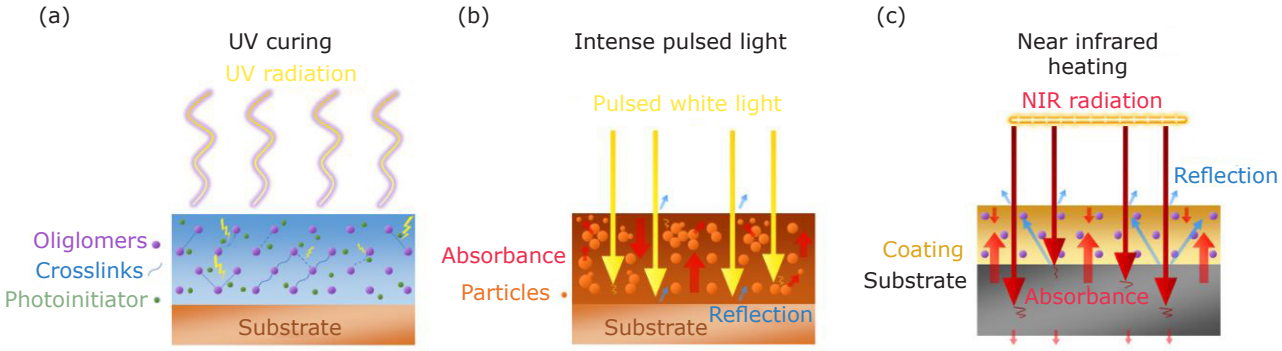

Fig. 2. Interaction of radiation with materials and substrate for: (a) UV curing; (b) IPL; (c) NIR heating

an organic coating (14). Commercially produced NIR adsorbing pigments are also specifically engineered for this purpose.

With traditional infrared (IR) heating it can be noted that the temperature achieved by the material being processed is not directly related to the energy required, for example a fan assisted oven at 100°C can utilise more energy per minute than an IR at 400°C (15) due to the high air flow requirement. In this case there can often be as much energy saved by using fast sintering techniques in place of low temperature air driers as there are for high temperature applications. By removing solvent quickly, the cost of re-condensing that solvent is reduced because there is a smaller volume of air to cool, resulting in further cost savings.

2. Techniques

2.1 Near Infrared Heating

Of the technologies discussed, NIR operates at the longest wavelength in the range of 700–1500 nm with the peak spectral output usually between 800–1200 nm. The lamps are typically tungsten–halogen filaments (16) and the emitted spectrum is dependent upon the power setting of the lamp. Heating the material is dependent on how the material absorbs the emitted radiation and the thickness of the material (16). The effect of reducing the lamp's power output on the emission spectra is shown in **Figure 3(a)**, where reduced lamp power moves the lamp output towards the higher wavelengths (18). This means that the energy imparted to the material is not a linear relationship with lamp power. The power output from a single lamp ranges from 6 kW for laboratory sized emitters to over 250 kW per emitter in steel coating lines (16). Maximum temperatures that can be achieved are dependent upon the lamps' energy density (in the range of 1200 kW m^{-2}) and the materials to be heated. Typical working temperatures are up to 800°C (19), however machines are available that can heat materials >1000°C, for example, the adphosNIR® 6 x 6 kW ceramic based NIR machine.

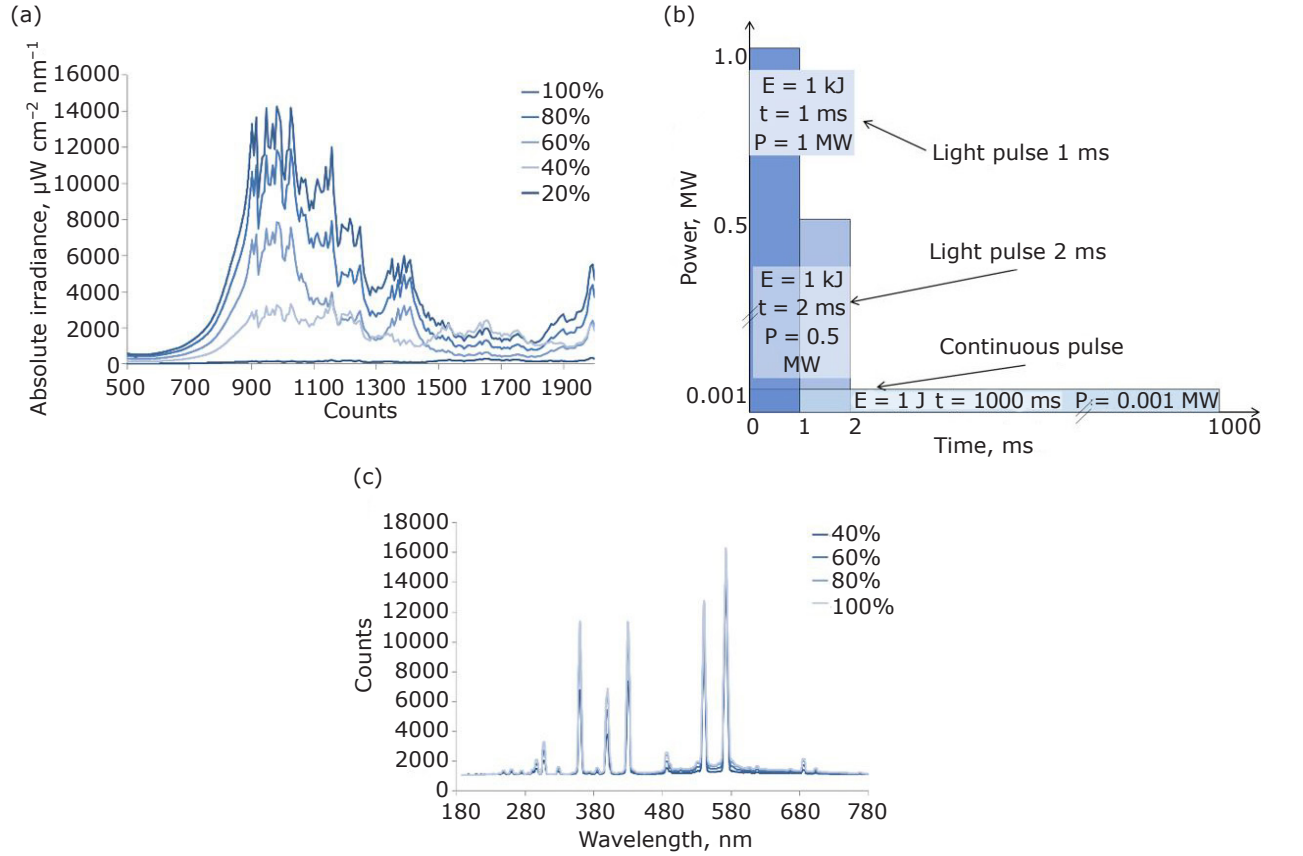

Fig. 3. (a) Absolute irradiance *vs*. wavelength for an adphos NIR lamp at different power outputs; (b) power delivered by continuous light and light pulses of different duration, having equal energy content. Reprinted from (17), Copyright (2005), with permission from Elsevier; (c) absolute irradiance *vs*. wavelength for a UV lamp at different power outputs

2.2 Intense Pulsed Light

IPL, also known as photonic or flashlight, involves the use of an inert gas lamp (such as xenon) which converts short duration and high-power electric pulses into radiation. Millisecond (or shorter) pulses of light from a xenon lamp are produced by applying high voltage and current between two tungsten electrodes through an inert xenon gas which generates an arc plasma. A super charged capacitor is used to deliver high electrical current in a short time (milliseconds). Xenon is most widely used because it is the most efficient gas to convert the applied electrical energy to white light. The spectrum of the lamp ranges as broad as UV to NIR (150–2500 nm) but the majority is in the visible region, where conversion is 50% in the range 200–1000 nm.

The power provided by pulses of light is greater than if the same equivalent total energy was provided by continuous light. The shorter the duration of the pulse, the higher the pulse power (**Figure 3(b)**), allowing a much higher penetrating capability through the material compared to continuous light (20). Crucially the short duration of light pulses also reduces the time available for thermal conduction inside the material, as well as other processes such as oxidation. This enables very rapid heating of a thin layer to much higher temperatures than the equivalent total energy not pulsed, without significantly increasing the temperature of the bulk (20).

The benefits of intense pulsed light combined with the high absorption of metal in the visible region has lent photonic to the application of curing printed circuits on visibly transparent, polymeric substrates which cannot withstand high temperatures. As described by Kinney *et al*. in their 1969 patent (21), brief intense pulses of light directed onto a printed pattern composed of conducting metal or semiconducting metal precursor can be converted to an electrical circuit pattern adhered to the substrate. "The heat profile of the composite element are such that the circuit is formed and energy dissipated before the substrate can be charred or decomposed, allowing heat sensitive substrates to be used" (21).

2.3 Ultraviolet Radiation

UV radiation operating at wavelengths of 240–580 nm (**Figure 3(c)**) is utilised in the laboratory, with 365 nm being the most common (peak) wavelength employed. This is mostly implemented using mercury UV lamps. When electricity is passed through the mercury vapour in the lamp the excitation causes UV light to be emitted, with the wavelength being dependent on the pressure.

UV curing can be used to tailor the cross-linking and porosity of a material, often enhancing the conductivity of the chosen material without deterioration (3, 22). This was shown by Zhang *et al*. where the conductivity of a polyethylene(oxide)-based solid polymer electrode was improved after UV curing compared with conventional heating (23).

The irradiation of a photopolymer *via* UV curing can cause photoinitiated chain growth and photoinduced crosslinking (**Figure 4**) *via* free radical photopolymerisation, initiated by free radicals formed from photoinitiators (PIs). PIs generate active species either through unimolecular dissociation or bimolecular photoinduced electron transfer reactions upon exposure to UV or visible light (3, 25, 24).

By adjusting the light intensity or concentration of photosensitive compounds, the rate of initiation

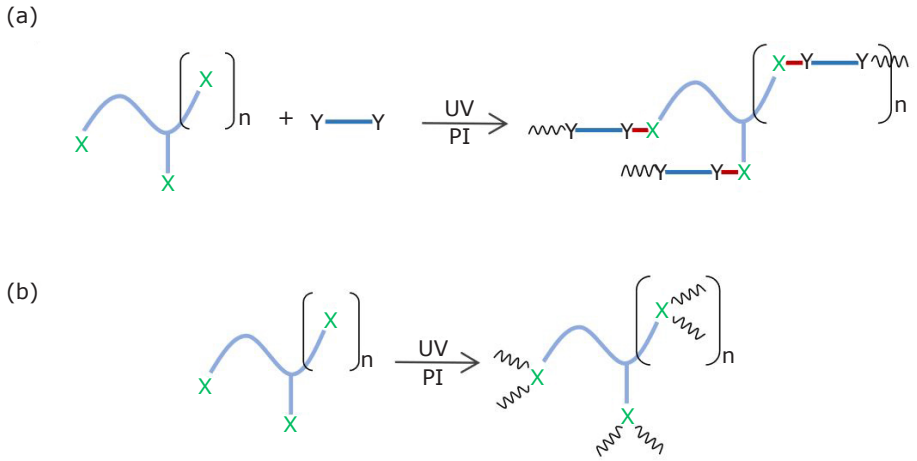

Fig. 4. Free radical photopolymerisation mechanisms: (a) crosslinking mechanism; (b) chain growth mechanism Reprinted with permission from (24). Copyright 2014 American Chemical Society

and polymerisation can be controlled. However, photoinitiated free radical polymerisation can be inhibited by oxygen which reacts with the carbon free radicals. In some cases UV curing of a material is performed in an inert environment (26, 27) to avoid this effect. The polymerisation process, in some materials, can also lead to reduced strength and increased brittleness unless prevented through the addition of additives or alterations to curing time (24, 25).

3. Applications in Photovoltaics, Batteries, Thermoelectrics and Fuel Cells

The requirement of the heating source is dependent upon the material transformation that is needed. Several material transformations are considered: sintering, binder removal, chemical reaction and drying (**Figure 5**). Because binder removal is commonly linked to sintering of a printed paste this will be considered within the sintering section that follows.

3.1 Sintering

The highest energy is typically needed for sintering where powder particles of either metal (27) or metal oxide (28) densify at a temperature lower than the melting point of the materials (**Figure 5**). The role of the binder is to provide structure to the paste and the correct rheology so that it can be printed, and to adhere the active material to the substrate if the particles are not going to be sintered (29). In the case of sintering, heat and oxygen cause the binder to be burnt leaving the material to be sintered behind. In some specialist cases such as NIR of carbon materials in perovskite solar cells (30) the carbon is not sintered but it is still key to remove the binder to ensure good charge transfer between the active materials, with even small amounts (<1 wt%) of binder having a catastrophic impact on performance. Adhesion is provided by the active perovskite material.

In the more typical case, such as in sintering titania pastes for dye-sensitised solar cells (DSSCs), the binder is removed first and then sintering occurs. The speed of processing limits grain growth and phase transformation even at temperatures exceeding 700°C (19). Titania for DSSCs has also been processed using photonic sintering (31) but since the fluorine doped tin oxide (FTO) substrate does not absorb in the visible region, NIR is often more effective since the substrate does absorb and enables heating of the titania (13, 19). Feleki *et al*. (32) compared binder and binder free titania paste sintered with thermal treatment, UV/O_3 (PR-100 UVIKON, NorthStar Scientific, UK) and photonic (PulseForge® 1300, NovaCentrix, USA). Photonic sintering was not able to fully remove the binder for the binder containing titania films but treating a commercial binder-free titania paste with 10 pulses of 2 ms enabled an average stabilised efficiency of 16.7% on indium tin oxide (ITO) glass and 12.3% on flexible ITO polyethylene naphthalate (PEN) (32). Sandmann *et al*. used UV-laser sintering on semiconductors zinc oxide and titania nanoparticle thin films, for applications such as DSSCs. A helium-cadmium-laser (UV-laser) at a wavelength of 325 nm was focused onto the specimen with a 40 mm lens and a 10 µm focal point diameter. This demonstrates that laser sintering can be observed

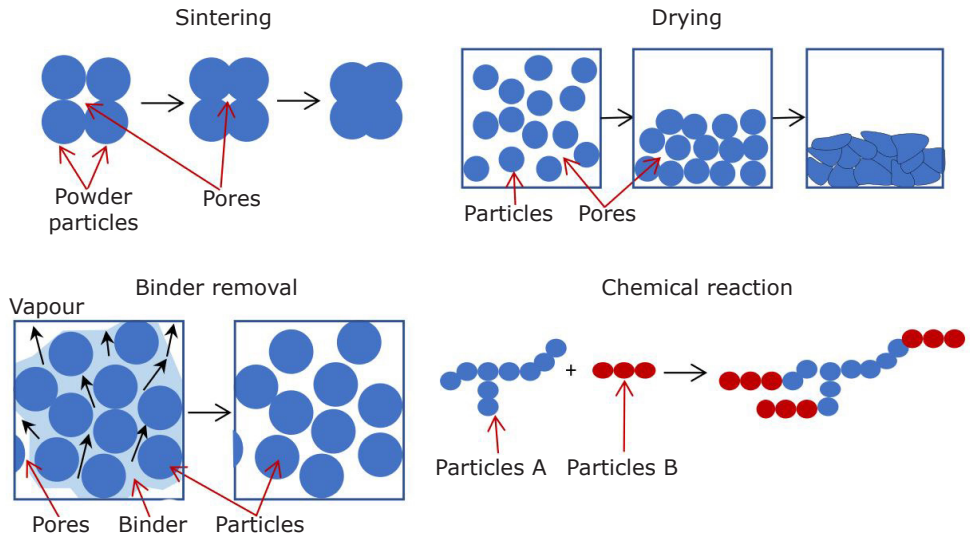

Fig. 5. Schematic of sintering, binder removal, chemical reaction and drying

even at laser powers as low as 30 mW, although the small spot size does not lend itself for mass production (33). Titania nanoparticles have been chemically sintered together using UV irradiation of a titania-titanium(IV) bis(ammonium lactate) dihydroxide (TALH) ink (34). The UV radiation causes photodegradation of the TALH to form new titania enhancing the connectivity among the original titania nanoparticles in the photoelectrode.

Bismuth telluride films for thermoelectric application have also been successfully sintered by Danei *et al*. using IPL in milliseconds on glass and polyimide films (35). Dharmadasa *et al*. processed 1 µm thick cadmium telluride films (36) using IPL to produce films of high density with grain sizes up to 1 µm. Their follow up paper (37) processed cadmium sulfide layers, used for cadmium telluride solar cells. The research demonstrated higher crystallinity than conventional sintering, attributed to the faster heating time and the change in temperature gradient across the sample. Dhage *et al*. (38) fabricated copper indium gallium diselenide (CIGS) solar cells from copper indium gallium and selenium nanoparticles under IPL without the need for a toxic, vacuum based selenisation step and opening the possibility for preparation of CIGS solar cells on temperature sensitive substrates without requiring a vacuum based process.

When sintering metallic printed circuits such as copper (39, 40), silver (41) and nickel (42) much of the research has been focused on using IPL. The inks are often based on metallic nanoparticle suspensions and can include polyvinylpyrrolidone to help stabilise the nanoparticles. The size of the nanoparticles can influence both their optical and thermal properties (43). In the case of nickel, it was found that uniform diameter 60 nm nickel nanoparticles could not be sintered alone, whereas a range of nickel nanoparticles with varying diameters (5–500 nm) could be sintered. This was due to the relatively narrow absorption range of 200–650 nm for 60 nm diameter particles, while 200 nm diameter particles have resonance peaks from 650 nm to 1000 nm. The range of different sizes greatly increased the absorption range of the nanoparticles, which allowed a better match with the lamp spectrum of 380–1000 nm and therefore they could more efficiently absorb the light and reach greater temperatures (42). Galagan *et al*. also used photonic sintering for their inkjet-printed silver grids (an alternative electrode to expensive ITO for organic solar cells) and obtained the same resistivity in 5 s compared with 6 h of oven sintering (44). Galagan demonstrated the photonic sintered grids had a sharper geometry resulting in decreased shadowing losses within the solar cell.

Tuning the wavelength of the radiation has been another method to improve the absorption of the material. Hwang *et al*. used various light filters to refine the wavelength of their xenon lamp (45). The copper films were most efficiently sintered using a band pass filter (from 500–600 nm) which aligned well to the peak absorption wavelength of 590 nm, see **Figure 6**.

NIR is utilised less for sintering metal nanoparticles than IPL due to less overlap in lamp emission and metal nanoparticle absorption. However, NIR has been used successfully to reduce the sintering time of silver nanoparticles on polyethylene terephthalate (PET) substrate to 12.5 s, slower than IPL but a significantly reduced time compared with IR sintering of gold and silver nanoparticles (46, 47).

3.2 Chemical Reaction and Curing

Radiative heating to initiate a chemical reaction is commonly seen during UV curing, involving the irradiation of polymers to form crosslinked network polymers. Commercial inks are available that have been developed for this purpose. Krebs *et al*. examined metal printed back electrodes for organic polymer solar cells that can be applied in a roll-to-roll process using UV-curable silver-based inks. Silver flakes and a UV-curable binder (EBECRYL®, allnex, Germany) were mixed, screen printed and UV cured for the solar cell. Results showed current extraction was efficient over the full area of the solar cell that was coated in silver, and increased current in areas coated in silver compare to those without (48).

UV-curing *in situ* is often used to solve the solid-solid interface contact problem caused by the conventional assembly process in the layer-by-layer fabrication of solid state batteries. In the case of *in situ* photopolymerisation the fluidity of the monomer allows the electrolyte precursor to penetrate the microporous structure of the electrode, allowing a strong adhesion to form with the electrode after polymerisation and greatly reducing the interfacial resistance (4). Kim *et al*. investigated the fabrication of bipolar all-solid-state lithium-sulfur batteries (ASSLSBs) *via* a UV curing-assisted stepwise printing process (2). Fabrication involved the ethyl methyl sulfone gel electrolyte, which incorporated a sulfur cathode paste being printed onto the desired object and subsequently solidified by exposure to UV irradiation. The tetraethylene glycol dimethyl ether gel composite

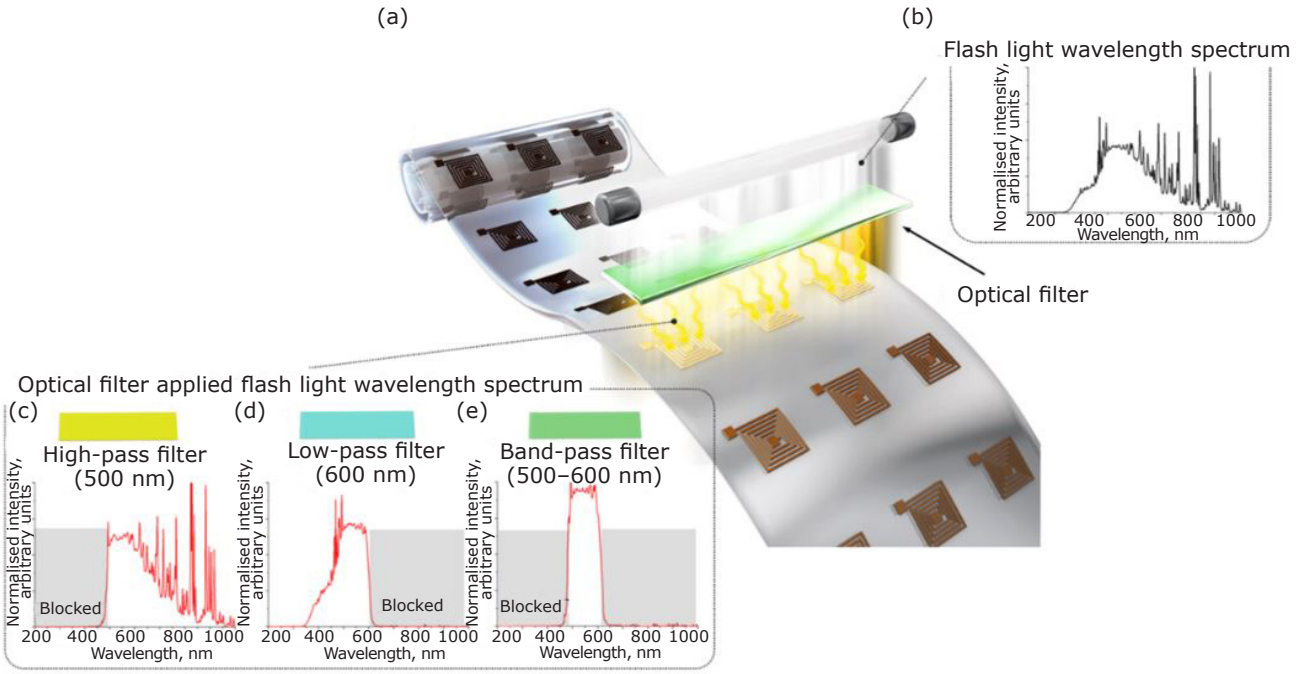

Fig. 6. (a) Schematics of the optical filter applied flashlight sintering system; (b) wavelength spectrum of the flashlight without filter; (c) wavelength spectrum of the flashlight with 500 nm high-pass filter; (d) wavelength spectrum of the flashlight with 600 nm low-pass filter; (e) wavelength spectrum of the flashlight with 500–600 nm band-pass filter. Reprinted with permission from (45). Copyright 2016 American Chemical Society

electrode was then added to the assembly and cured by the same process; the lithium metal anode was then placed on top to create an ASSLSB unit cell. This printing and UV curing process was repeated to create a bipolar ASSLSBs structure with two thermodynamically immiscible gel electrolytes in the printed battery (2). This ASSLSB showed high cycling performance with a discharge capacity of 680 mAh g^{-1} after 200 cycles.

Yang *et al*. used similar technology to prepare solid polymer electrolytes (SPEs) for all-solid-state LIBs (ASSLIBs) *via* UV curing using a one-step process. The electrolyte was UV-cured *in situ* on the cathode using a UV lamp, facilitating free radical photo-polymerisation to create the three-dimensional (3D) polymer network structure (4). The electrolyte had three components: the $(ethylene\ glycol)_9$ methyl ether acrylate (mPEGA) matrix, ethoxylated trimethylolpropane triacrylate (ETPTA) cross linker and succinonitrile (SN) additive. Crosslinking of ETPTA and mPEGA *via* UV curing formed a 3D network. The polyacrylate backbone provided mechanical strength, while the amorphous polyethylene oligomer side chains facilitate the transport of lithium ions. The SN additive (uniformly distributed in the crosslinked network) accelerated ion transport by promoting the dissociation of the lithium salts (4). Characterisation indicated the cathode layer and the SPE layer were tightly coupled without visible delamination, and the polymer was successfully crosslinked. The *in situ* polymerisation of the electrolyte on the electrode reduced the interfacial resistance and polarisation, as well as demonstrating an improved electrochemical performance than equivalent conventional ASSLIBs (4).

Similarly, Imperiyka *et al.* investigated the performance of solid-state ion conducting polymer electrolytes, but instead as an application for DCCSs. The polymer electrolytes were formulated from poly(glycidyl methacrylate) in the presence of a photoinitiator 2,2-dimethoxy-2-phenylacetophenone. UV curing allowed the linear polymers to form rapidly and trap the redox couples, which is favourable in PV conversion devices. A homopolymer structure was formed which facilitated charge transport and ionic migration. In this research the conductivity of the linear polymer electrolytes was good compared to traditional processes (for example, thermal treatments and catalysed reactions) (22).

UV curing can also be utilised in proton exchange membranes (PEM) for fuel cell applications. Rao *et al*. applied the technique for Nafion® PEMS in

micro-direct methanol fuel cells, irradiated the PEM at wavelengths between 240–450 nm. Nafion® PEMs consist of hydrophobic fluorocarbon backbone chains with perfluoroether side chains containing some strong hydrophilic sulfonic acid groups (3). The optimal dose of UV irradiation was determined by studying the membrane samples water uptake, swelling ratios, porosity and conductivity. Rao demonstrated that increasing the dose of UV radiation increased the proton conductivity, reaching an optimal dose of 198 mJ cm^{-2} (3). The UV irradiation created crosslinking with the PEMs to form more hydrophilic sulfonic acid functional groups, in turn tuning the porosity of the Nafion® membranes and increasing the proton conductivity (which doubled at that optimal UV dose). Polarisation plots also showed significant improvements in voltage as well as power density (3).

Other forms of radiation induced chemical reaction include perovskite crystallisation (Equation (i)) which has been achieved using both photonic sintering (49) and NIR (50). The absorber layer in perovskite solar cells, which is composed typically of methyl ammonium lead iodide or similar and absorbs strongly in the visible region, lends itself well to photonic processing. The heating rate must be controlled to ensure dense crystallisation and to avoid the evaporation of methyl ammonium iodide leaving lead iodide (Equation (ii)) rather than lead halide perovskite.

$$CH_3NH_3I(dmf) + PbI_2(dmf) \rightarrow CH_3NH_3PbI_3(s) \quad (i)$$

$$CH_3NH_3I(dmf) + PbI_2(dmf) \rightarrow CH_3NH_3I(g) + PbI_2(s) \quad (ii)$$

The first photonic processing of perovskite films was demonstrated by Troughton *et al*. (49). They used a PulseForge® 1300 to flash anneal spin coated $CH_3NH_3PbI_{3-x}Cl_x$ perovskite films on alumina/FTO glass. The mesoporous alumina acted as a scaffold layer for the perovskite where some perovskite film is embedded within it and there is a capping layer of perovskite on top. Perovskite films heated by 1.15 ms of photonic exposure had a poorer performance in solar cells than the standard films heated for 90 min on a hot plate (up to 11.3% compared to 15.2%) which was likely due to the capping layer becoming ejected and removed in places due to the near instantaneous phase transformation (49). Lavery *et al*. reported perovskite solar cells using photonic annealing of $CH_3NH_3PbI_3$ perovskite films made from the two-step deposition approach on titania/FTO glass (51). This involves depositing a PbI_2 film first (which they heated on a hot plate at 100°C for 5 min) and then dipping the film into a solution of CH_3NH_3I in isopropanol to convert the PbI_2 to perovskite. This was then exposed to flash white light to grow the perovskite crystals. With increasing white light pulse energy the cubical particles grew and became a dense compact film (**Figure 7**) (51). In this work the crystals were already nucleated and were being grown, whereas in the previously mentioned work (49) the film needed both nucleation and crystallisation and there would have been residual solvent in the film.

3.3 Drying

Drying operations primarily involve evaporating solvents, although they can also aid film densification

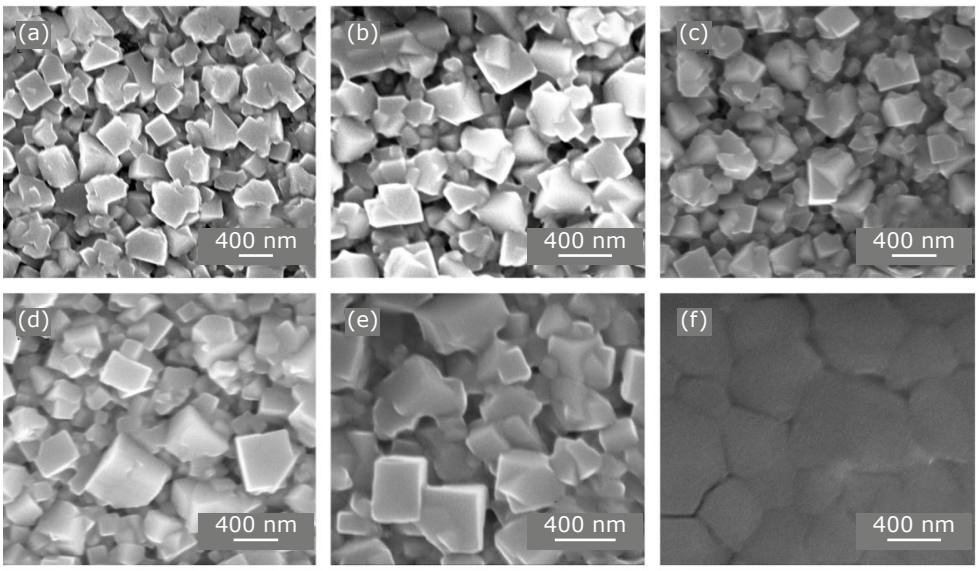

Fig. 7. Top view scanning electron microscopy images of perovskite films: (a) without IPL exposure; (b) after a 2 ms pulse of IPL exposure at 1000 J $pulse^{-1}$; (c) after a 2 ms pulse of IPL exposure at 1250 J $pulse^{-1}$; (d) after a 2 ms pulse of IPL exposure at 1500 J $pulse^{-1}$; (e) after a 2 ms pulse of IPL exposure at 1750 J $pulse^{-1}$; (f) after a 2 ms pulse of IPL exposure at 2000 J $pulse^{-1}$. Reprinted with permission from (51). Copyright 2016 American Chemical Society

and improved conduction as demonstrated by Potts *et al*. (52) when IPL drying conductive carbon inks, which are used in many energy applications. Drying of the conducting polymer polyethylenedioxythiophene with polystyrene sulfonic acid (PEDOT:PSS) can be undertaken more quickly by NIR than by conventional methods. As the PEDOT:PSS dries the film becomes more transparent to NIR, reducing the potential to overheat the PET substrate (28). An additional advantage to rapid heating technologies is that they have a more concentrated solvent in the exhaust, which is then easier to recondense and recycle since the volume of air being cooled is smaller.

4. Practical Considerations

All radiative technologies suffer from a difficulty in measuring the exact temperature which the material being processed experiences. Thermocouples can be soldered to the surface of the substrate being processed (19) but inaccuracies are caused should the thermocouple react differently to the radiative heating compared with the substrate, and should be taken as comparative measurements within identical geometries rather than absolute values. For substrates where it is not possible to solder a thermocouple, for example glass, an IR camera can be used. When using an IR camera it is essential calibration is undertaken at exactly the same set up (such as camera angles) as for the actual measurement as described by Hooper (53). Roy *et al*. (54) when microwave sintering used both optical pyrometers and sheathed thermocouples close to the sample to measure temperatures and whilst these could give comparative readings within +/–5°C they could not confirm the actual temperature so precisely.

If the material contains a component which decomposes near the processing temperature (such as a polymeric binder) a temperature can be approximated, as in the case of Baker *et al*. (30) where thermal gravitational analysis was used to quantify remaining binder after sintering of a carbon cathode. Since binder removal was also time and energy input dependent it was not a quantitative assessment. Brennan (16) utilised heat equations to calculate temperature of spectrally selective surface coatings on any substrate material with good agreement to the experimental data of steel coating products.

In addition to difficulties determining the precise working temperature, there can be negatives to the fast heating rate with respect to thermal stresses. In cases where the material is not uniformly coated internal cracking may be initiated due to thermal stresses within the substrate, **Figure 8**. To mitigate this (if slower heating does not work) systems can be set up with multiple inline lamps to provide a preheat, heat and then post-heat such that cooling can be controlled and thermal cracking avoided. A simpler solution can be to use a substrate carrier that also absorbs the heating radiation to help reduce the thermal stresses within the substrate.

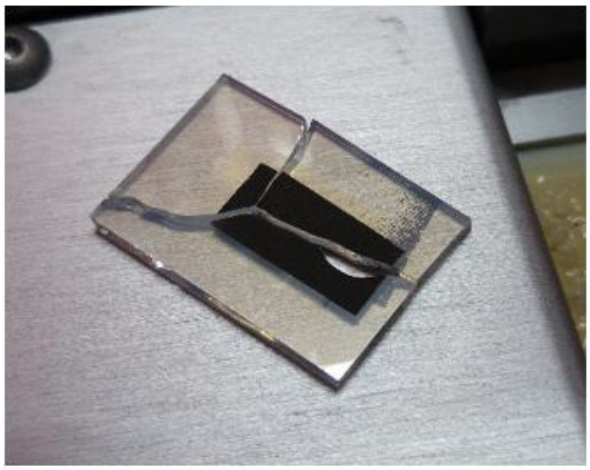

Fig. 8. Glass substrate with carbon coating after NIR has heated the carbon preferentially to the glass and caused thermal cracking

The rapid heating of inks with solvent remaining can also cause defects such as solvent boil (16, 28). The steel coating industry has highlighted this issue with some of their coatings noting this could be solved by using coatings designed with the right absorption properties, specifically for NIR processing (16). Huang *et al*. (55) demonstrate the importance not only of the absorbance of the substrate but also of the solvent when designing for NIR, with butanol showing particularly strong absorbance within the NIR wavelengths.

5. Summary

Radiative heating technologies have been embraced by industry to reduce processing times and energy input. However, some of the key advantages of these techniques have not been fully exploited. The precision of heating such that the coating can be sintered whilst the substrate remains cool is a key advantage in the field of printed electronics. But it has other advantages in that it can reduce diffusion between two reactive layers and enable component architectures not possible with conventional heating technologies. It is hoped that this study encourages material scientists to consider radiative response during their design of coatings in order to take advantage of these techniques, not just for efficient heating, but for new energy device designs.

Glossary

ASSLIB	All-solid-state lithium-ion battery
ASSLSB	All-solid-state lithium-sulfur battery
CIGS	Copper indium gallium diselenide
DSSC	Dye-sensitised solar cell
ETPTA	Ethoxylated trimethylolpropane triacrylate
FTO	Fluorine doped tin oxide
IPL	Intense pulsed light
IR	Infrared
ITO	Indium tin oxide
LIB	Lithium-ion battery
mPEGA	(ethylene glycol)$_9$ methyl ether acrylate
NIR	Near infrared
PEDOT:PSS	Polyethylenedioxythiophene with polystyrene sulfonic acid
PEM	Proton exchange membrane
PEN	Polyethylene naphthalate
PET	Polyethylene terephthalate
PI	Photoinitiator
PV	Photovoltaic
SN	Succinonitrile
SPE	Solid polymer electrolyte
TALH	Titanium(IV) bis(ammonium lactate) dihydroxide
UV	Ultraviolet

Acknowledgements

This work was supported by the Engineering and Physical Sciences Research Council (EPSRC) through ECR Fellowship NoRESt (EP/S03711X/1) and SPECIFIC Innovation and Knowledge Centre (EP/N020863/1 and EP/P030831/1). The authors would like to acknowledge the M2A funding from the European Social Fund *via* the Welsh Government (c80816), the Engineering and Physical Sciences Research Council (Grant Ref: EP/S02252X/1) that has made this research possible.

Declaration of Interest

adphos GmbH are a project partner on EP/S03711X/1 but were not involved in the writing of this document.

References

1. "Net Zero – The UK's Contribution to Stopping Global Warming", Committee on Climate Change, London, UK, May, 2019, 275 pp
2. S.-H. Kim, J.-H. Kim, S. J. Cho and S.-Y. Lee, *Adv. Energy Mater.*, 2019, **9**, (40), 1901841
3. A. S. Rao, K. R. Rashmi, D. V. Manjunatha, A. Jayarama, S. Prabhu and R. Pinto, *Int. J. Hydrogen Energy*, 2019, **44**, (42), 23762
4. Z. Yang, Y. Luo, X. Gao and R. Wang, *ChemElectroChem*, 2020, **7**, (12), 2599
5. K. Mizushima, P. C. Jones, P. J. Wiseman and J. B. Goodenough, *Mat. Res. Bull.*, 1980, **15**, 783
6. A. Kojima, K. Teshima, Y. Shirai and T. Miyasaka, *J. Am. Chem. Soc.*, 2009, **131**, (17), 6050
7. M. M. Lee, J. Teuscher, T. Miyasaka, T. N. Murakami and H. J. Snaith, *Science*, 2012, **338**, (6107), 643
8. J. Baker, D. Deganello, D. T. Gethin and T. M. Watson, *Mater. Res. Innov.*, 2014, **18**, (2), 86
9. M. Hösel, R. R. Søndergaard, M. Jørgensen and F. C. Krebs, *Energy Technol.*, 2013, **1**, (1), 102
10. J. Park, K. Shin and C. Lee, *Int. J. Precis. Eng. Manuf.*, 2016, **17**, (4), 537
11. J. Perelaer, R. Abbel, S. Wünscher, R. Jani, T. Van Lammeren and U. S. Schubert, *Adv. Mater.*, 2012, **24**, (19), 2620
12. M. Oghbaei and O. Mirzaee, *J. Alloys Compd.*, 2010, **494**, (1–2), 175
13. K. Hooper, M. Carnie, C. Charbonneau and T. Watson, *Int. J. Photoenergy*, 2014, 953623
14. I. Mabbett, J. Elvins, C. Gowenlock, C. Glover, P. Jones, G. Williams and D. Worsley, *Prog. Org. Coatings*, 2014, **77**, (2), 494
15. J. A. Alberola-Borràs, J. A. Baker, F. De Rossi, R. Vidal, D. Beynon, K. E. A. Hooper, T. M. Watson and I. Mora-Seró, *iScience*, 2018, **9**, 542
16. D. A. Brennan, 'A Computational and Experimental Study on Near-Infrared Heating for the Coil Coating Industry', Swansea University, Swansea, UK, 2018
17. L. Palmieri and D. Cacace, 'High Intensity Pulsed Light Technology', in "Emerging Technologies for Food Processing", ed. D.-W. Sun, Ch. 11, Elsevier, 2005
18. C. Cecile, K. Hooper, M. Carnie, J. Searle, B. Philip, D. Wragg, T. Watson and D. Worsley, *Prog. Photovolt.: Res. Appl.*, 2014, **22**, (12), 1267
19. M. J. Carnie, C. Charbonneau, P. R. F. Barnes, M. L. Davies, I. Mabbett, T. M. Watson,

B. C. O'Regan and D. A. Worsley, *J. Mater. Chem. A*, 2013, **1**, (6), 2225

20. J. E. Dunn, R. W. Clark, J. F. Asmus, J. S. Pearlman, K. Boyer, F. Painchaud and G. A. Hofmann, Maxwell Laboratories Inc, 'Methods for Preservation of Foodstuffs', *US Patent* 4,871,559; 1989
21. L. C. Kinney and E. H. Tomkins, Monsanto Company, 'Method of Making Printed Circuits' *US Patent* 3,451,813; 1969
22. M. Imperiyka, A. Ahmad, S. A. Hanifah and F. Bella, *Phys. B: Condens. Matter*, 2014, **450**, 151
23. Y. Zhang, W. Lu, L. Cong, J. Liu, L. Sun, A. Mauger, C. M. Julien, H. Xie and J. Liu, *J. Power Sources*, 2019, **420**, 63
24. J. V. Crivello and E. Reichmanis, *Chem. Mater.*, 2014, **26**, (1), 533
25. X. Pan, M. A. Tasdelen, J. Laun, T. Junkers, Y. Yagci and K. Matyjaszewski, *Prog. Polym. Sci.*, 2016, **62**, 73
26. J. R. Nair, C. Gerbaldi, M. Destro, R. Bongiovanni and N. Penazzi, *React. Funct. Polym.*, 2011, **71**, (4), 409
27. S. Wünscher, R. Abbel, J. Perelaer and U. S. Schubert, *J. Mater. Chem. C*, 2014, **2**, (48), 10232
28. D. Bryant, I. Mabbett, P. Greenwood, T. Watson, M. Wijdekop and D. Worsley, *Org. Electron.*, 2014, **15**, (6), 1126
29. F. Jeschull, D. Brandell, M. Wohlfahrt-Mehrens and M. Memm, *Energy Technol.*, 2017, **5**, (11), 2108
30. J. Baker, K. Hooper, S. Meroni, A. Pockett, J. McGettrick, Z. Wei, R. Escalante, G. Oskam, M. Carnie and T. Watson, *J. Mater. Chem. A*, 2017, **5**, (35), 18643
31. H.-J. Hwang and H.-S. Kim, *J. Nanosci. Nanotechnol.*, 2015, **15**, (7), 5028
32. B. Feleki, G. Bex, R. Andriessen, Y. Galagan and F. Di Giacomo, *Mater. Today Commun.*, 2017, **13**, 232
33. A. Sandmann, C. Notthoff and M. Winterer, *J. Appl. Phys.*, 2013, **113**, (4), 044310
34. Y. Oh, S.-N. Lee, H.-K. Kim and J. Kim, *J. Electrochem. Soc.*, 2012, **159**, (10), H777
35. R. Danaei, T. Varghese, M. Ahmadzadeh, J. McCloy, C. Hollar, M. S. Saleh, J. Park, Y. Zhang and R. Panat, *Adv. Eng. Mater.*, 2019, **21**, (1), 1, 1800800
36. R. Dharmadasa, B. Lavery, I. M. Dharmadasa and T. Druffel, *ACS Appl. Mater. Interfaces*, 2014, **6**, (7), 5034
37. R. Dharmadasa, I. M. Dharmadasa and T. Druffel, *Adv. Eng. Mater.*, 2014, **16**, (11), 1351
38. S. R. Dhage, H.-S. Kim and H. T. Hahn, *J. Electron. Mater.*, 2011, **40**, (2), 122
39. H.-S. Kim, S. R. Dhage, D.-E. Shim and H. T. Hahn, *Appl. Phys. A*, 2009, **97**, (4), 791
40. S.-H. Park, W.-H. Chung and H.-S. Kim, *J. Mater. Process. Technol.*, 2014, **214**, (11), 2730
41. D. J. Lee, S. H. Park, S. Jang, H. S. Kim, J. H. Oh and Y. W. Song, *J. Micromechanics Microengineering*, 2011, **21**, (12), 125023
42. S.-H. Park and H.-S. Kim, *Thin Solid Films*, 2014, **550**, 575
43. O. A. Yeshchenko, I. M. Dmitruk, A. A. Alexeenko and A. M. Dmytruk, *Phys. Rev. B*, 2007, **75**, (8), 085434
44. Y. Galagan, E. W. C. Coenen, R. Abbel, T. J. Van Lammeren, S. Sabik, M. Barink, E. R. Meinders, R. Andriessen and P. W. M. Blom, *Org. Electron.*, 2013, **14**, (1), 38
45. Y.-T. Hwang, W.-H. Chung, Y.-R. Jang and H.-S. Kim, *ACS Appl. Mater. Interfaces*, 2016, **8**, (13), 8591
46. D. Tobjörk, H. Aarnio, P. Pulkkinen, R. Bollström, A. Määttänen, P. Ihalainen, T. Mäkelä, J. Peltonen, M. Toivakka, H. Tenhu and R. Österbacka, *Thin Solid Films*, 2012, **520**, (7), 2949
47. A. Denneulin, A. Blayo, C. Neuman and J. Bras, *J. Nanoparticle Res.*, 2011, **13**, (9), 3815
48. F. C. Krebs, R. Søndergaard and M. Jørgensen, *Solar Energy Mater. Solar Cells*, 2011, **95**, (5), 1348
49. J. Troughton, M. J. Carnie, M. L. Davies, C. Charbonneau, E. H. Jewell, D. A. Worsley and T. M. Watson, *J. Mater. Chem. A*, 2016, **4**, (9), 3471
50. J. Troughton, C. Charbonneau, M. J. Carnie, M. L. Davies, D. A. Worsley and T. M. Watson, *J. Mater. Chem. A*, 2015, **3**, (17), 9123
51. B. W. Lavery, S. Kumari, H. Konermann, G. L. Draper, J. Spurgeon and T. Druffel, *ACS Appl. Mater. Interfaces*, 2016, **8**, (13), 8419
52. S.-J. Potts, Y. C. Lau, T. Dunlop, T. Claypole and C. Phillips, *J. Mater. Sci.*, 2019, **54**, (11), 8163
53. K. E. A. Hooper, 'Rapid Processing of Dye-Sensitised Solar Cells Using Near Infrared Radiative Heating', PhD Thesis, Swansea University, UK, 2014
54. R. Roy, D. Agrawal, J. Cheng and S. Gedevanlshvili, *Nature*, 1999, **399**, (6737), 668
55. S.-H. Huang, C.-K. Guan, P.-H. Lee, H.-C. Huang, C.-F. Li, Y.-C. Huang and W.-F. Su, *Adv. Energy Mater.*, 2020, **10**, (37), 2001567

The Authors

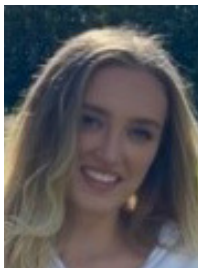

Rebecca Griffin is a first year PhD candidate studying at the University of Swansea, UK. Her passion for sciences started during her BSc Hons and MSc by Research degrees at Lancaster University, UK, in Natural Science with a focus in chemistry. Her current research interests are within the field of energy storage, specialising in solid-state batteries, electrochemistry and photochemistry.

Katherine Hooper is a postdoctoral researcher in printed photovoltaics at Swansea University. Her PhD 'Rapid Processing of Dye-Sensitised Solar Cells using Near Infrared Radiative Heating' was awarded in 2014. Her current research activities focus on scale-up of solid-state solar cells, both perovskite and organic technologies.

Cecile Charbonneau and her team focus on the development of nanomaterials and processes for the fabrication of compact and porous semiconductor metal oxide layers. She favours a low-carbon footprint approach (aqueous precursors, low-temperature processing, roll-to-roll compatible deposition methods) to enable the commercialisation of novel products in the fields of third-generation photovoltaics and water purification based on the use of these advanced coatings.

Jenny Baker joined academia from the aerospace industry in 2011 to undertake a PhD, 'Flexographic Printing of Graphene Catalysts to Replace Platinum', at the Welsh Centre for Printing and Coating, UK. Following this she undertook a postdoctoral position in solid state printed perovskite solar cells, focusing on sustainable manufacturing methods and materials. She is currently the electrochemical storage lead for SPECIFIC, Swansea University, working on storage solutions for non-mobile applications and is an EPSRC ECR Fellow.